Nepheloid Layers in the deep Gulf of Mexico

Wilford D. Gardner
Department of Oceanography, Texas A&M University, College Station, TX 77843 USA.
ORCID # 0000-0002-6299-3744

Mary Jo Richardson
Department of Oceanography, Texas A&M University, College Station, TX 77843 USA,
ORCID # 0000-0001-9583-139X

Alexey V. Mishonov
CISESS/ESSIC/University of Maryland, NCEI/NOAA affiliate, Silver Spring, MD, 20910 USA, ORCID # 0000-0002-2958-8747

Daniel A. Bean
Shell International Exploration & Production, Houston, TX 77079, USA.

Juan Carlos Herguera
Division of Oceanology, CICESE, Center for Scientific Research and Higher Education at Ensenada, Ensenada, Baja California, Mexico, ORCID # 0000-0001-8335-2607

*Corresponding author: Wilford D. Gardner: wgardner@ocean.tamu.edu, P: 1-979-845-3928
Texas A&M University, College Station, TX 77843, USA. ORCID # 0000-0002-6299-3744

Highlights:

1. Beam c_p data reveal weak to very strong nepheloid layers in the deep Gulf of Mexico.
2. Loop Current eddies and other currents may create varying bottom nepheloid layers.
3. Bottom currents create mega-furrows and nepheloid layers at Sigsbee escarpment base.
4. Nepheloid layers were weak in the deep Yucatan Channel and Straits of Florida.

Abstract

The first measurements of bottom nepheloid layers in the central and southern deep waters of the Gulf of Mexico west of the Yucatan peninsula were made during the three summers of 2015-2017. Particulate matter concentrations (PM) were estimated from optical profiles of beam attenuation due to particles (c_p). Near-bottom maps and vertical sections of c_p and PM converted from c_p show evidence of sediment resuspension, possibly linked with topographic Rossby waves, loop current eddies, or eddy-topography interactions. Additional c_p profiles were made along cross-slope transects around the entire Gulf of Mexico, including across the Yucatan Channel and Straits of Florida in 2017. Near-bottom PM concentrations were barely elevated in the deep Yucatan Channel and Straits of Florida at that time, except in about the surface 200 m along the northern and western boundaries. Comparison was made between areas with benthic nepheloid layers and Eddy Kinetic Energy (EKE) patterns in the deep Gulf of Mexico. Regions of high EKE or strong bottom currents in the central and eastern Gulf were found over a large region of deeply eroded furrows in the seafloor previously imaged using 3-D seismic profiling and submersible observations. Few PM measurements were obtained in the high EKE areas during these expeditions, however, historical and recent sampling show very strong nepheloid layers at stations within and westward of the region of the actively eroding furrows.

Key Words:
Gulf of Mexico
Nepheloid layers
Transmissometer beam attenuation
Bottom furrows
Current erosion
Eddy Kinetic Energy

1. Introduction

Global distribution of bottom nepheloid layers shows connections between high surface eddy kinetic energy (EKE) or mean kinetic energy (MKE) with strong bottom nepheloid layers resulting from resuspension of bottom sediments (Gardner et al., 2017; 2018b). Those syntheses did not include bottom nepheloid layers in the deep Gulf of Mexico due to lack of in-situ data. While high EKE has been previously observed in the eastern Gulf (Dixon et al., 2011; Wunsch, 2015; Perez-Brunius et al., 2018), synchronous particulate matter measurements in the water column were not made. Many studies of particle distribution and nepheloid layers in the Gulf have been made on the shelf and slope down to 1000-1500 m (e.g. Shideler, 1981; Zhang, 1997; Bernal, 2001; Cochran, 2013, Zuck, 2014; Gray, 2016; Diercks et al., 2018), but fewer data have been available to evaluate nepheloid layers in the deep (>1500 m) Gulf of Mexico until recently.

High resolution 3-D seismic data have also revealed the presence of large-scale furrows at the base of some portions of the Sigsbee Escarpment (Bryant et al., 2001; Bean, 2005). Studies have measured strong currents near some of the furrowed regions in the Gulf (Hamilton & Lugo-Fernandez, 2001; Bean, 2005), but there were no simultaneous measurements of PM concentrations in the vicinity of those furrows. However, new measurements from a 2021 survey show high particle concentrations in the furrows area.

New beam attenuation data from five cruises that had a variety of different scientific objectives have been uniformly processed and compared with other published data to understand the potential relationships outlined above.

The purposes of this paper are:

1) To map the distribution of particulate matter in the nepheloid layers in the deep Gulf of Mexico and some adjacent shelf/slope regions.
2) To explore spatial relationships between loop-current eddies (Tenreiro et al., 2018) or eddy kinetic energy (Perez-Brunius et al., 2018) throughout the Gulf of Mexico with
    a) new beam attenuation data showing the distribution of bottom nepheloid layers in the deep Gulf, and
    b) erosional furrows along the base of the Sigsbee Escarpment in the northern Gulf (Bryant et al., 2001; Bean, 2005).
3) To test for the presence of nepheloid layers in the Yucatan Channel and the Straits of Florida that might indicate sediment transport through those passages.

2. Background

2.1 Gulf of Mexico Basin

A physiographic map of the Gulf of Mexico (Figure 1) shows two major carbonate platforms, each bounded by steep escarpments, two slope regions sculpted by rising salt domes and other gravitational downslope processes, and an abyssal plain deeper than 3000 m. The Mississippi River provides sediment that creates a large shelf delta and a deep-sea fan (Coleman, 1988; Davis, 2017). The Mississippi Canyon traps and transports sediment that erodes the canyon and builds up the Mississippi Fan. Rivers in Mexico deliver sediment to the Gulf of Campeche in the southern Gulf of Mexico (Davis, 2017).

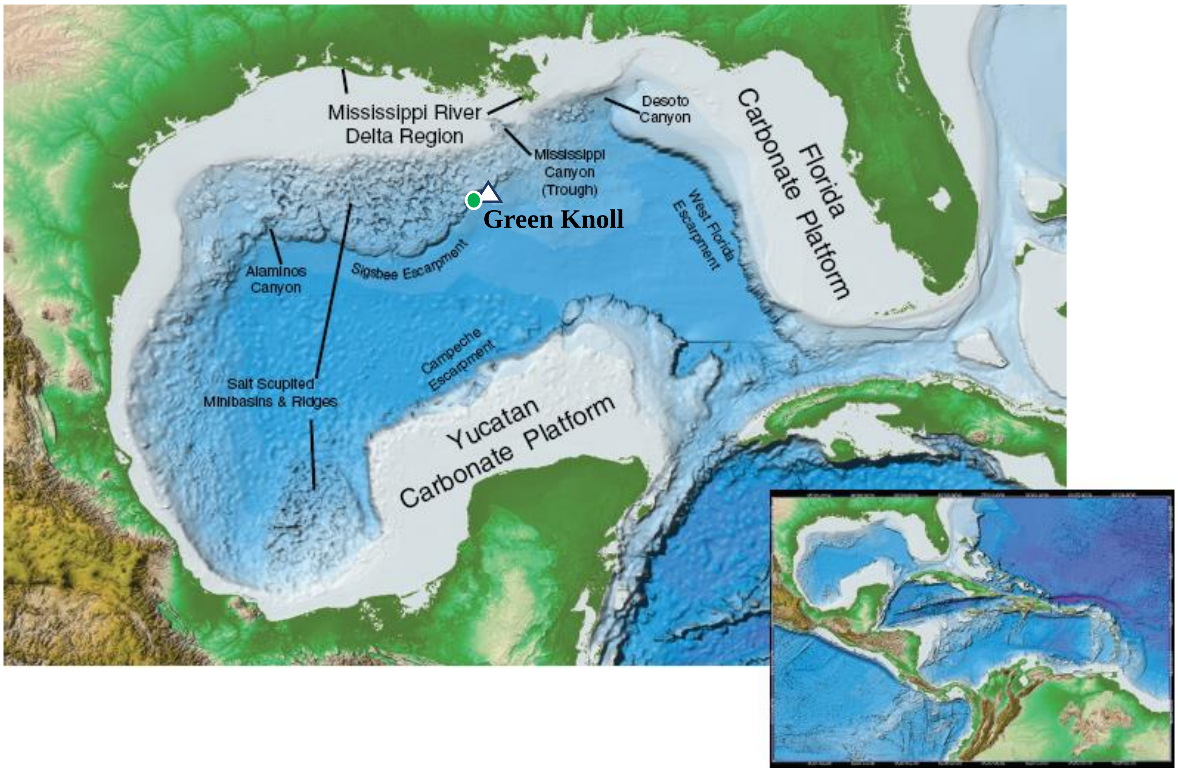

Figure 1. Physiographic map shows two major carbonate platforms with steep escarpments, two areas of salt-sculpted mini-basins and ridges molded by rising salt domes bordered seaward by steep escarpments, and the abyssal plain deeper than 3000 m. (Modified from National Academies of Sciences, Engineering, and Medicine, 2012). The green dot at the base of the Sigsbee escarpment marks Green Knoll. Current measurements were made northeast of Green Knoll by Hamilton & Lugo-Fernandez, 2001 (white triangle).

2.2. Gulf of Mexico Hydrography

Perez-Brunius et al., (2018) review the dominant circulation patterns in the Gulf of Mexico. They view the Gulf as a highly stratified basin with a two-layer system. The upper layer (shallower than 800-1000 m) has surface-intensified flows. The lower layer (>1200 m to the seafloor) shows that currents do not depend on depth, and are dominated by topographic Rossby waves (Hamilton, 2009). Flow in the upper layer is dominated by the Loop Current

(LC), which enters the Gulf through the Yucatan Channel between Mexico and Cuba, advects water masses into the northern Gulf, meanders clockwise east, then back south and exits the Gulf through the Straits of Florida (Figure 2). This meandering loop in the Gulf expands and contracts depending on the transport through the Yucatan Channel and the detachment of large anticyclonic eddies from the LC (Oey et al. 2005). After exiting the Gulf, the flow turns north and mixes with water feeding the Gulf Stream, a prominent western boundary current along the east coast of North America (National Academies of Sciences, Engineering, and Medicine, 2018).

Within the Gulf, the LC sheds large (~200-300 km in diameter) anticyclonic eddies at irregular time intervals between 4 and 12 months (Leben, 2005). The anticyclonic eddies are often times associated with cyclonic/anticyclonic eddies on its edges (Figure 2). These energetic Loop Current Eddies (LCE) drift slowly towards the western Gulf, dissipating their energy along the way (DiMarco et al., 2005; Kolodziejczyk, 2012; Hamilton et al., 2014). Observations show how these LCEs shape the upper slope by generating strong currents along the 200 m isobath (Maslo et al., 2020).

Perez-Brunius et al. (2018) note that the circulation in the deep Gulf waters is less well known, but cite several studies suggesting that the LC and associated large mesoscale eddies can influence the dynamics of the bottom waters below 1000 m. Those studies suggest there is a mean cyclonic flow around the deep basin, and that the expansion and contraction of the LC induces movement in the lower layer via baroclinic instabilities, deep eddies, and topographic Rossby waves (TRWs) to both the interior and northern boundary of the western basin.

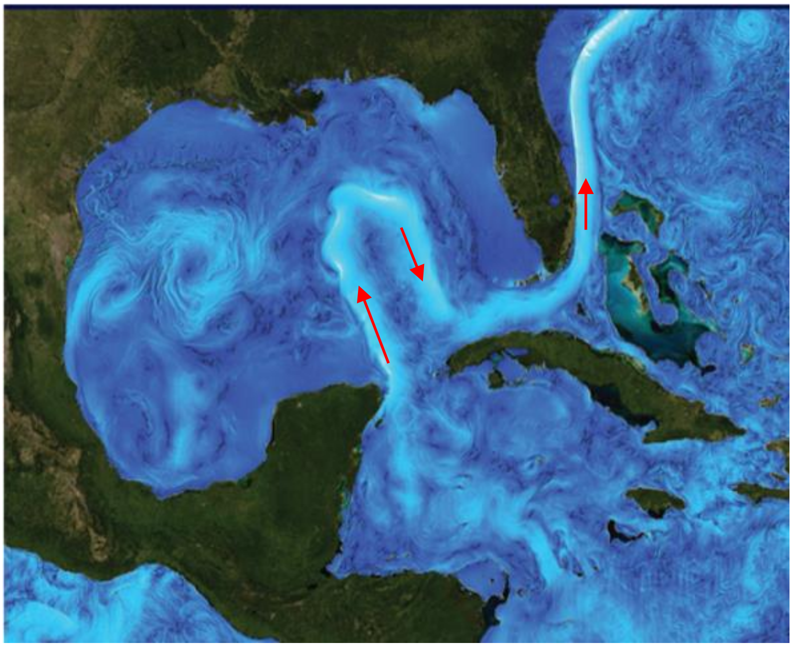

Figure 2. Surface circulation in the Gulf of Mexico shows water entering through the Yucatan Channel (light blue and red arrows), showing a well-developed Loop Current circulation in the Gulf and its outflow through the Straits of Florida. Cyclonic and anticyclonic Loop Current eddies usually develop with the detachment of the Loop Current anticyclonic eddy and dissipate energy during a westward drift. (Modified from National Academies of Sciences, Engineering, and Medicine, 2018).

Hamilton and Lugo-Fernandez (2001) measured currents at several locations in the vicinity of the Sigsbee Escarpment (Figure 1). Currents were measured at 1600 m, 1800 m, and 1989 m (9 meters above bottom, a.k.a. mab, Figure 3) on a mooring in a water depth of 1998 m (white triangle in Figure 1) a few kilometers NE of Green Knoll. Currents showed reversing NE-SW flow velocities from near zero to >80 cm s^{-1} with a period of 10-14 days. They concluded that topographic Rossby waves with a period of 10-14 days controlled the dynamics in the lower water column with reversing currents varying from near zero to >80 cm s^{-1}, clearly sufficient to erode bottom sediments (Miller et al, 1977).

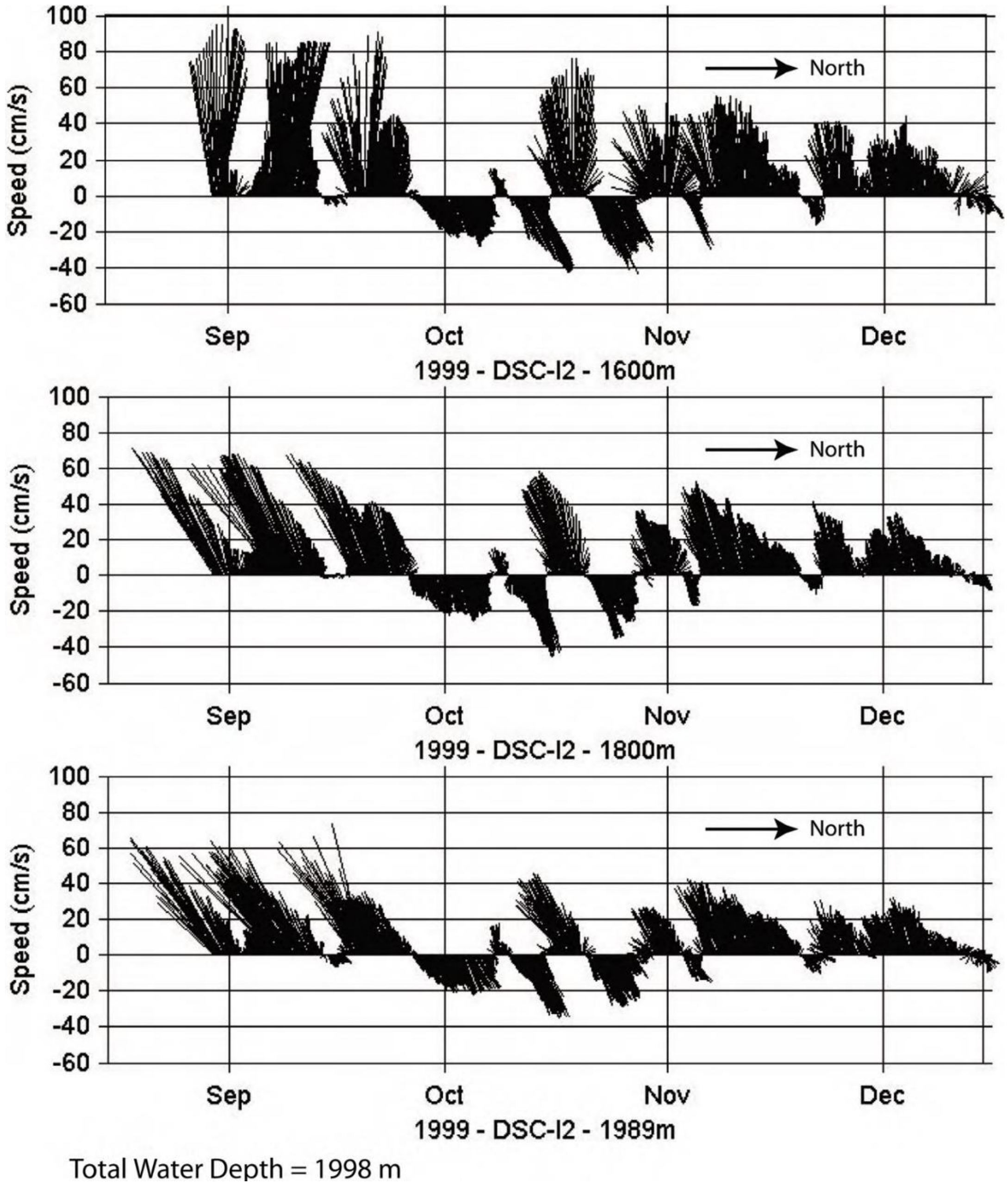

Figure 3. Current vectors measured at three depths by Hamilton & Lugo-Fernandez (2001, figure 3) at the location marked by white triangle in Figures 1 and 11. Note the rotated direction of North in comparing flow direction in Figure 11 map. Flow was NE-SW, roughly parallel with topographic contours. Figure from Bean (2005, figure 4). Data are also displayed as vector diagrams in Hamilton (2007, figure 3).

The strong currents measured by Hamilton & Lugo-Fernandez (2001) have also been linked with deep-sea mega furrows (Figure 4) discovered along the Sigsbee Escarpment (Bryant et al., 2001; Bean, 2005).

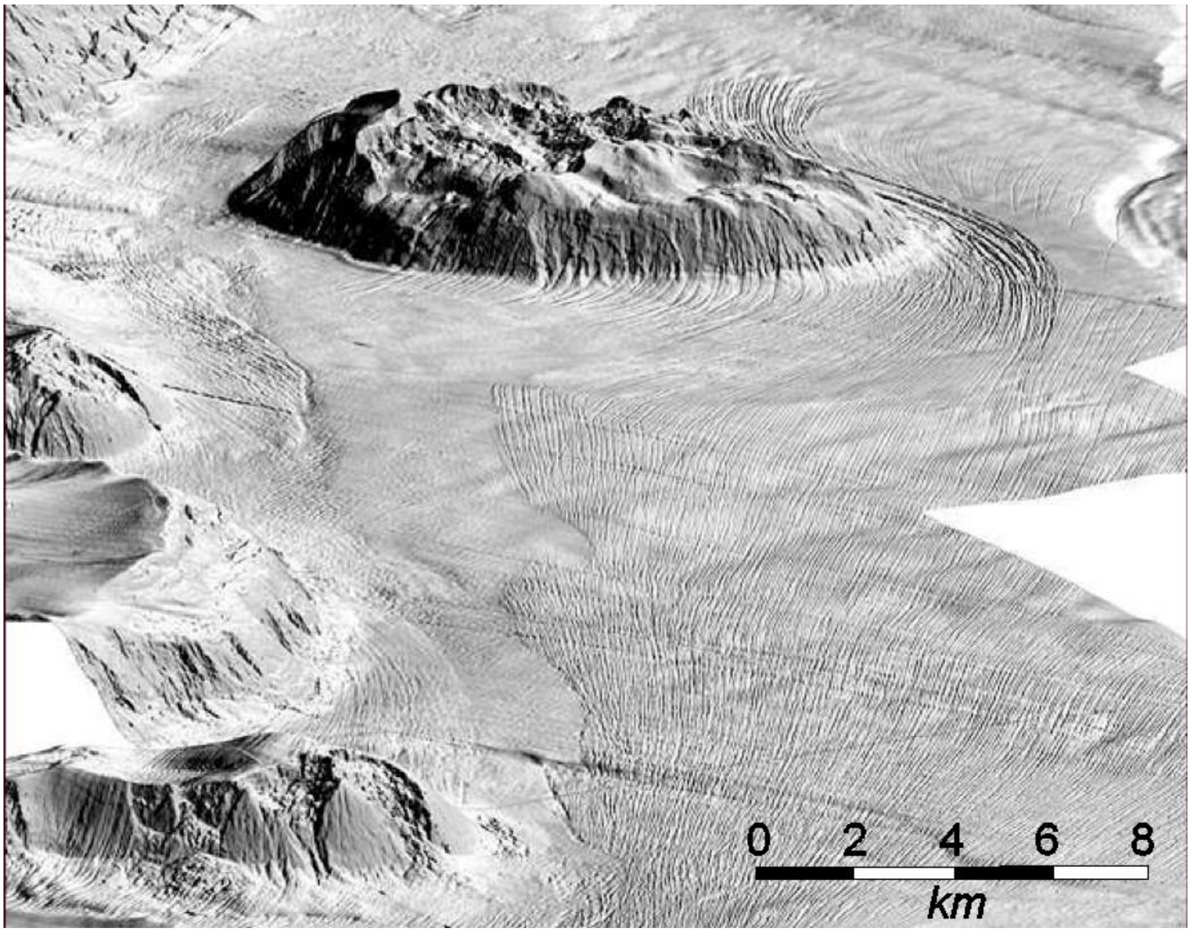

Figure 4. 3D seismic profiling reveals mega-furrows created by currents that are still active along the base of Sigsbee Escarpment in the vicinity of Green Knoll (modified from Bean, 2005; figure 5). Vertical exaggeration is ~4x. Green Knoll's location is denoted by the green dot in Figure 1 and a black dot in Figure 11. The c_p profile from Station 4-37 in Figure 9 with a maximum observed PM value of ~550 µg l^{-1} was made close to, and possibly in the furrow field.

There are numerous parallel furrows along the escarpment that vary between 1-10 m deep and range from 5-50 m wide (Bryant et al., 2001). Spacing between furrows is 20-200 m and they continue along the base of the escarpment for as long as 100 km and trend up, over, or around obstacles as large as Green Knoll, which is over 200 m in height. Direct observations and videos from Deep Sea R/V Alvin indicated the slope of the furrow walls ranged from nearly vertical to 45° and currents measured with an upward looking ADCP on the submersible were 30-50 cm s^{-1} in the furrowed region (Bean, 2005). The forces creating these furrows are still active, but it takes long periods of erosion to create and maintain these large-scale features.

The presence of a mean cyclonic flow around the deep basin was suggested by numerical studies (Bracco et al., 2016; Lee, 2003; Oey and Lee, 2002). This cyclonic flow was confirmed using an array of deep-water moorings in the western and southern Gulf of Mexico (Tenreiro et al., 2018).

Another significant observation of Perez-Brunius et al., (2018) is the very high eddy kinetic energy in the eastern Gulf, which matched findings of Dixon et al. (2011). During the hydrographic studies mentioned so far, there were no reported measurements of particle concentrations near the seafloor in the deep water column.

3. Sampling sites and methods

In this paper we will link sparse past measurements and new, recent optical measurements of beam attenuation converted to particle mass concentrations (PM) throughout the Gulf. The sampling strategies during the cruises on which these optical measurements were made were designed to study ocean acidification, biogeochemistry, and sediment cores, not nepheloid layers or currents, but the optical data obtained with transmissometers provide important new insights and gave a rare opportunity to learn more about nepheloid layers in the Gulf.

3.1 Station locations

In the summer/fall of 2015-2017, scientists aboard Mexico's research vessel B/O Justo Sierra collected CTD/transmissometer profiles during three expeditions occupying approximately the same sampling grid in the central and southern deep waters of the Gulf of Mexico (Figure 5, green dots). This research was conducted during project XIXIMI cruises 4, 5, & 6 (Linacre et al., 2019). In the summer of 2017, CTD/transmissometer profiles were also made along nine cross-slope transects around the Gulf of Mexico, plus across the Yucatan Channel and the south and north Straits of Florida during the GOMECC3 expedition on NOAA ship Ron Brown (Figure 5, red dots). Another expedition in September-October 2021 expanded the GOMECC3 station pattern and added a few new stations in deep waters seaward of the GOMECC3 lines (selected preliminary data became available to us, courtesy of the cruise PIs).

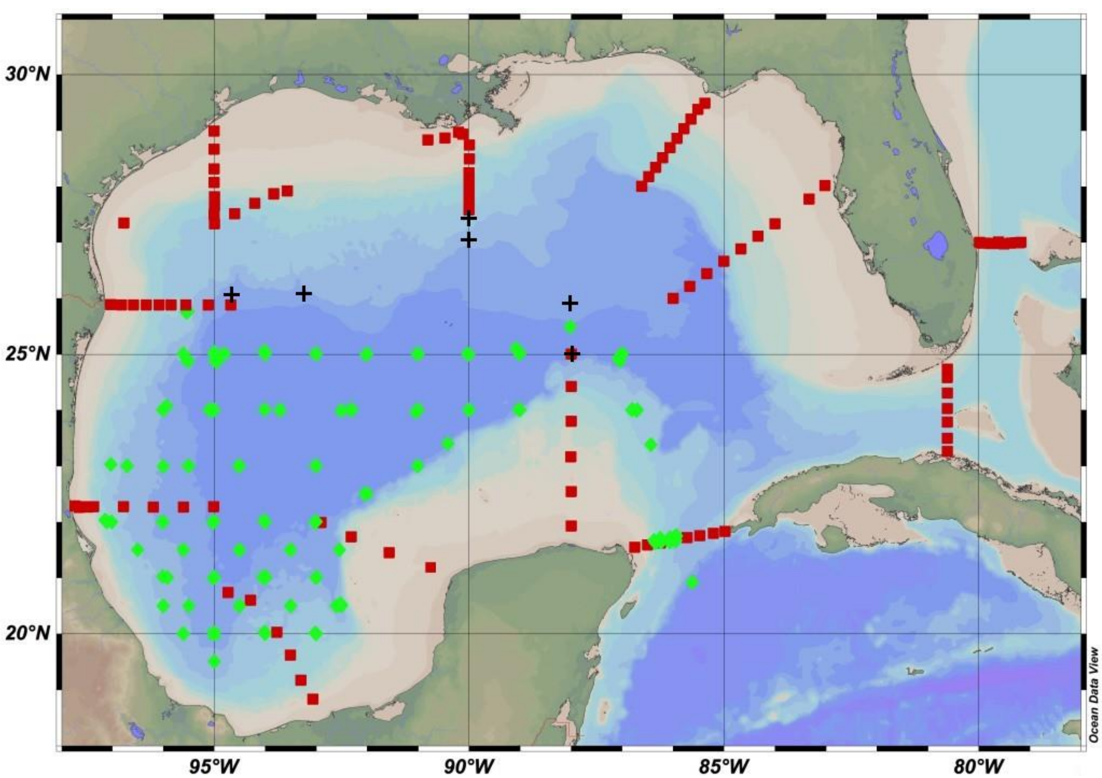

Figure 5. Station locations during Mexico's three B/O Justo Sierra surveys in summer/fall of 2015-2017 (green dots) and of NOAA's ship Ron Brown expedition in summer of 2017 (red dots), and six deep-water stations from 2021 (black crosses). The outer edge of light blue shading on the station map denotes 1000 m depth.

3.2 Transmissometer data

WetLabs 25-cm pathlength C-STAR transmissometers with a 650 nm LED light source were used to make all profiles. Transmissometers measure the transmission of light (*T*) across a path of known length (*r*) in volts (0-5 volts (V)). Voltage is then converted to beam attenuation of light (*c*) by the equation:

$$V/5 = T = e^{-cr}$$

which can be rearranged as

$$c = -(1/r) * ln (T)$$

Data processing included examination and removal of transient spikes, 2 db bin data averaging, determination of water column minimum value, and adjustments for LED drift based on factory and field air readings. Ideally, calibrations are also done using regressions of PM or particulate organic carbon concentrations (POC) versus *c*, but neither PM nor POC samples were collected concurrently with profiles used in these studies. Without in-situ samples it is not feasible to establish a definitive concentration at the minimum *c* in the water column. Thus, we applied the method of using the profile minimum voltage or a cruise-average minimum (for shallow profiles) on each cast. We later set the *c* minimum value to zero, so all values based on *c* are then due to particle concentrations greater than the profile minimum, c_p. Profiles of c_p (beam attenuation due to particles) are used in making water column sections of c_p and PM assessment. The near-bottom values of c_p are used to compile bottom maps. Details of data reduction and calibration methods are published in Gardner et al. (2018b).

Beam c_p is linearly correlated with particle concentration when the composition and size distribution are uniform (Baker and Lavelle, 1984). Because both of those variables change through the water column seasonally and regionally (e.g. Gardner et al., 2001), the particulate matter data are best visualized and interpreted using c_p. Filtration sampling by Brewer et al. (1976) and our own measurements in many oceans show minimum particle concentrations of ~5-12 µg l^{-1}.

An intensely-sampled area south of Nova Scotia, Canada, with a wide range of nepheloid layer concentrations (Gardner et al., 1985) produced a relation of c_p to PM in the bottom 100's of meters as follows:

$$PM\ (\mu g\ l^{-1}) = 1208 * c_p,\ r^2 = 0.94$$

This relationship was used for estimating particle concentration in global syntheses of bottom nepheloid layers (Gardner et al., 2017; 2018b). Using the above equation, PM value of 5-12 μg l^{-1} is equivalent to 0.004-0.010 units of c_p (m^{-1}).

Beam attenuation data were gridded and displayed using Ocean Data View (ODV) software (Schlitzer, R., 2021). Variations in c_p deeper than ~200 m are minimal through most of the water column unless intermediate or bottom nepheloid layers are encountered (Southard and Cacchione, 1972; McCave, 1986). CTD casts generally were lowered to 5-15 mab, though some profiles intentionally covered only the upper water column.

4. Results

4.1 Sections and seafloor maps of c_p (PM) distributions during XIXIMI 4, 5, & 6 cruises.

Vertical sections of c_p along 24°N during the three XIXIMI summer/fall cruises demonstrate an absence of a clear annual pattern of particle distribution. However, weak bottom nepheloid layers were always found in some region of the deep basin and a strong nepheloid layer occurred along the western margin of the Gulf in 2015 and 2016 (Figure 6 d, g). Some of the increased c_p values extend vertically hundreds of meters to over 1000 mab. Nepheloid layers were most intense and abundant in 2015 and least intense and abundant in 2017.

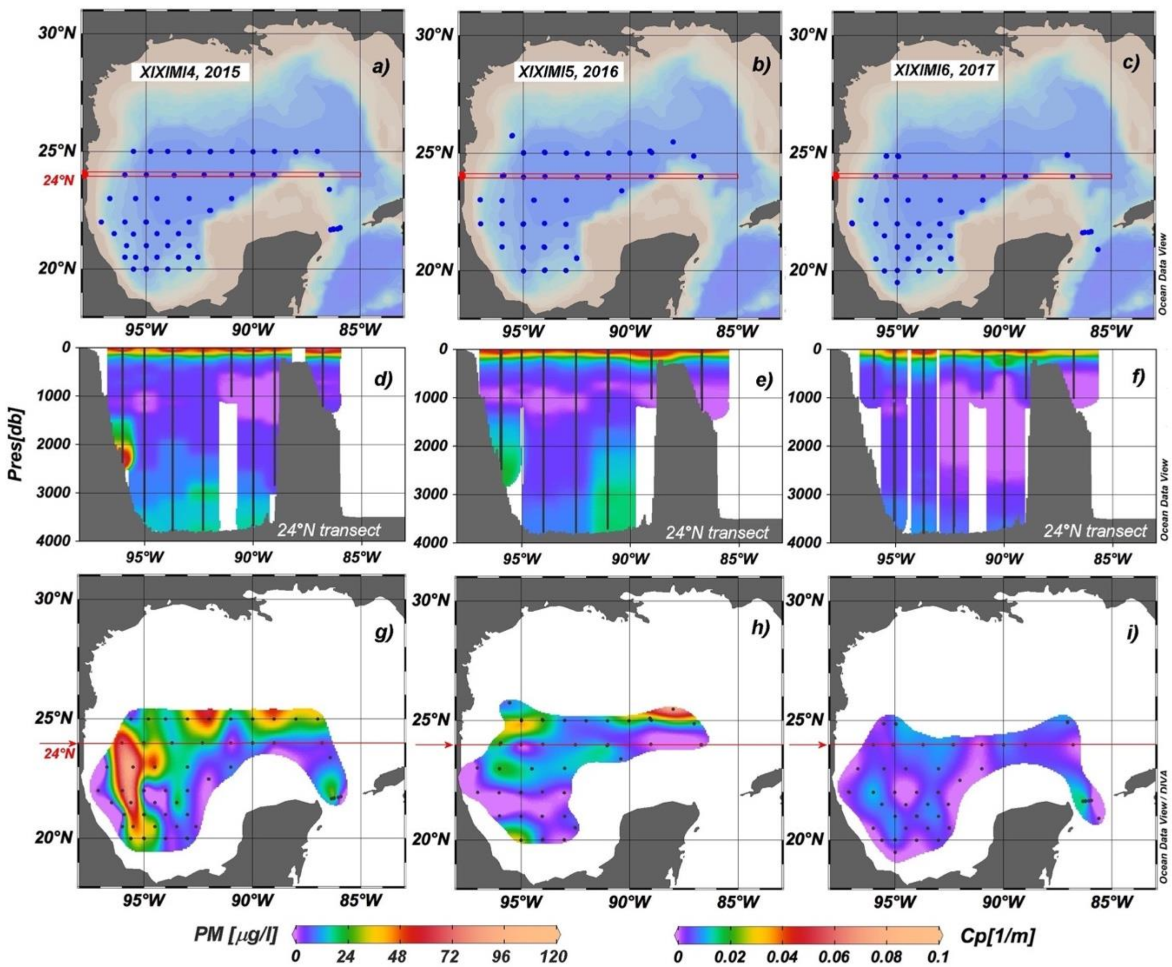

Figure 6. a-c) Station maps of c_p profiles during XIXIMI 4-6 cruises; d-f) vertical sections of c_p (m^{-1}) at stations between red lines in a-c) along 24°N in 2015-2017; g-i) maps of bottom c_p in 2015-2017. Arrows and red lines in g-i indicate the line of stations used for sections shown in d-f. Bold vertical lines in the sections (d-f) indicate the location of profiles. The outer edge of light blue shading on the station maps (a-c) denotes 1000 m depth.

4.2 Nepheloid layer distribution and concentration in the Gulf from all XIXIMI and GOMECC cruises.

While the three XIXIMI cruises (4, 5, and 6) primarily sampled the deep southern basin and not the surrounding shelf (Figure 6a, b, c), the GOMECC3 cruise produced nine cross-shelf-slope sections around the entire Gulf, plus across three channel/straits: Yucatan Channel, South Florida Strait and North Florida Strait (Figure 7a, b, red dots and profiles). With all of the XIXIMI6 and GOMECC3 (both 2017) profiles combined (Figure 7b – stacked c_p profiles from both expeditions), we obtain a broader picture of much of the Gulf in 2017. Shelf and upper slope c_p values can be five times to more than ten times greater than in the deep Gulf waters (Figures 6, 7). Note that these data provide just brief snapshots of water column profiles and bottom c_p values during three summers.

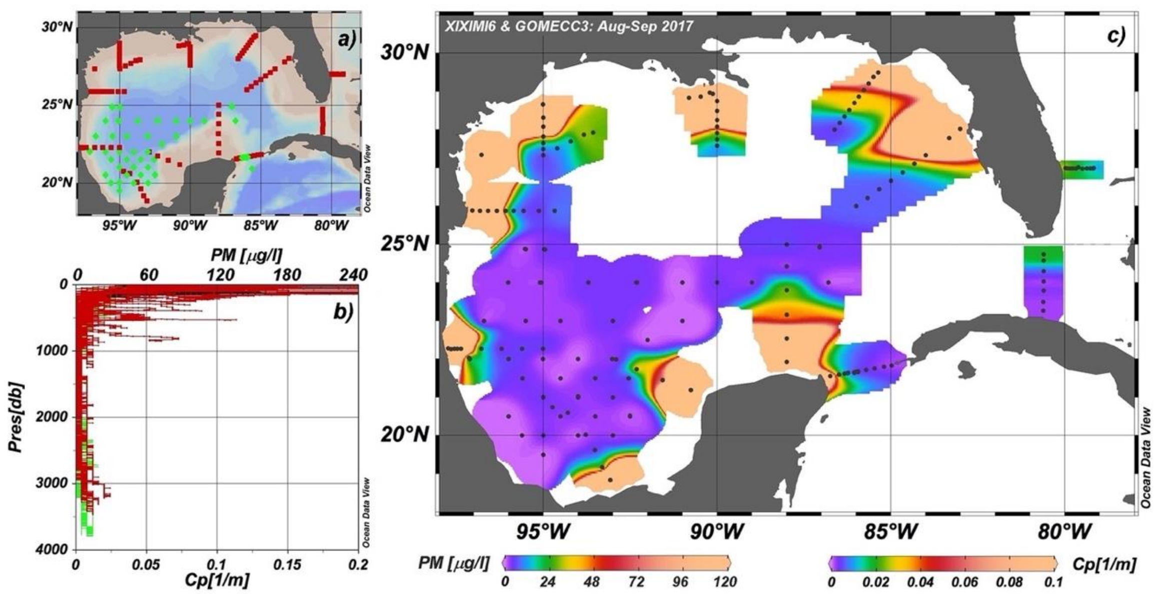

Figure 7. Station locations (a), profiles (b), and (c) map of bottom c_p (m^{-1}) during 2017 summer season based on combined XIXIMI6 (green) and GOMECC3 (red) data. The outer edge of light blue shading on the station map (a) denotes 1000 m depth.

Profiles from three pairs of stations occupied in both 2017 (GOMECC3) and reoccupied in 2021 (preliminary CTD data courtesy of cruise PIs) reveal significant PM differences between the two expeditions four years apart (Figure 8). Bottom temperature, salinity and density are nearly identical below 1200 m at all three overlapping stations observed four years apart, indicating homogeneous water in the deep Gulf. At the western station, c_p-based PM values are low in 2017 (Sta. 3-54, max ~25 μg l^{-1}), but extremely high in 2021 (Sta. 4-70, max ~440 μg l^{-1}). The central station's PM values at ~1200 m depth were also low (max ~15 µg l^{-1}) in 2017 (Sta. 3-22) and much higher (~120 µg l^{-1}) in 2021 (Sta. 4-38). PM concentrations at southeastern stations in both years were low; ~15 µg l^{-1} in 2017 (Sta. 3-64) and ~40 µg l^{-1} in 2021 (Sta. 4-104). None of the T, S, or density profiles showed any shifts at the depths where c_p increased.

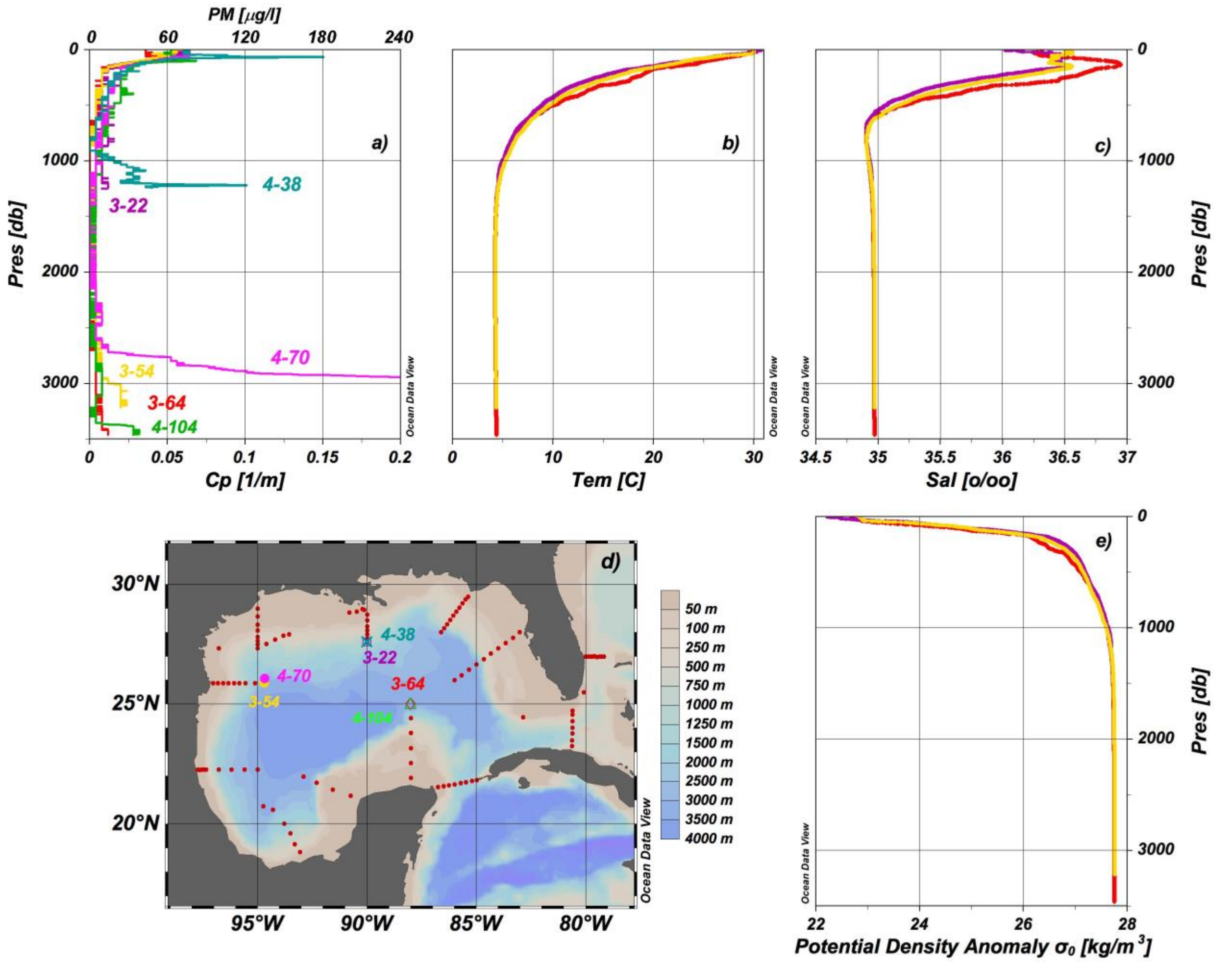

Figure 8. Profiles of c_p (a), T (b), S (c), and D (e) at the deepest stations of three transects occupied in 2017 (GOMECC3, labeled 3-xx) and at the same three locations in 2021 (labeled 4-xx) (colored symbols and labels in d). Red dots – GOMECC3 survey pattern.

A few additional stations were sampled during 2021. Profiles from those stations are shown in Figure 9 (preliminary data, courtesy of the PIs). Temperature, salinity and density are nearly identical below 1200 m at all three stations in 2021, similar to 2017 data. At the western station (4-73), seaward of the 2017 station 3-54, c_p was extremely high (max c_p>1.18, PM>~1400 µg l^{-1}). At the central station (4-37), c_p at ~2300 m depth (c_p>0.45, PM~550 µg l^{-1}) was near Green Knoll and was much greater than at other stations located further north along 90°N line where depths varied between 400 m to 1200 m (c_p = 0.01 to 0.06, PM~12 to 72 µg l^{-1-}: data from profiles used in Figure 7). PM concentration at the central eastern station (4-106) was also very high: ~550 µg l^{-1}, and was in an area of high kinetic energy (Perez-Brunius et al., 2018). None of the T, S, or density profiles showed any shifts at the depths where c_p increased. These three stations are shown as colored symbols in Figure 9.

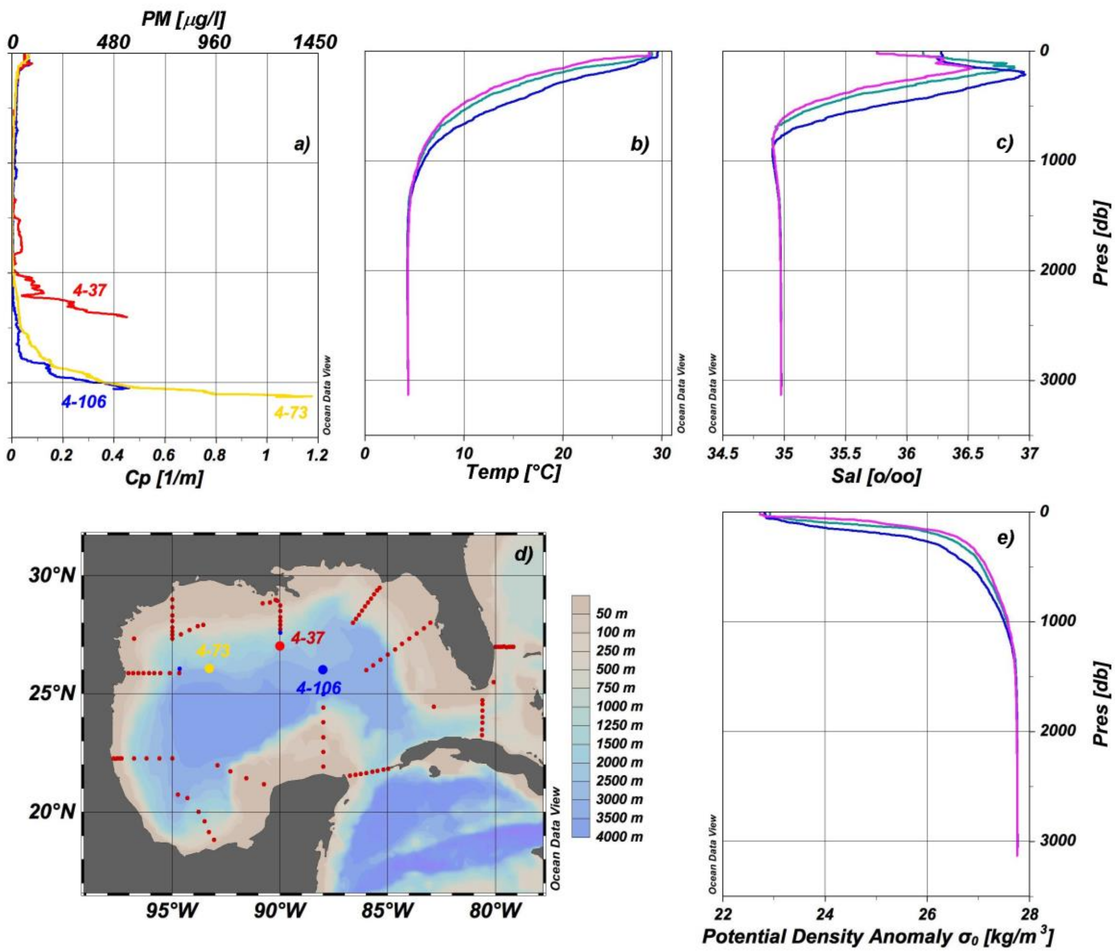

Figure 9. Profiles of c_p (a), T (b), S (c), and D (e) at three stations occupied in 2021 (colored symbols and labels in d). Red dots – GOMECC3 survey pattern. Note that the c_p and PM scales in a) are six times larger than the scale in Figure 8a.

4.3 Nepheloid layers in three straits

Data along full sections across the Yucatan Channel, South and North Florida Straits (Figure 10) were collected during 2017 and revealed only very weak nepheloid layers in the deepest regions, with low PM concentrations on the order of 10 μg l^{-1}. Concentrations in the upper 300-400 m of the two straits along the south and east Florida coast were about 100 μg l^{-1}.

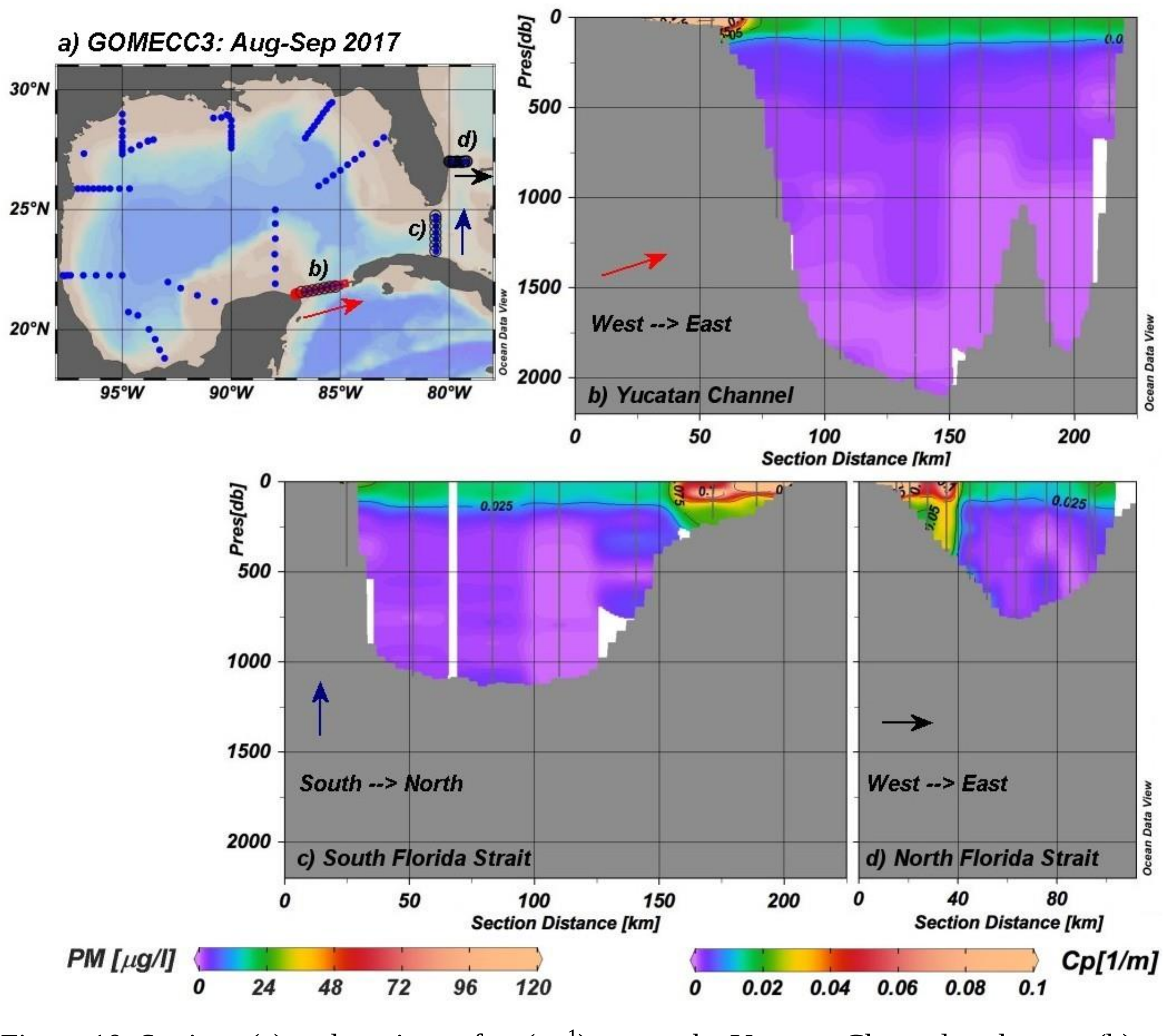

Figure 10. Stations (a) and sections of c_p (m^{-1}) across the Yucatan Channel, red arrow (b), South Florida Strait, blue arrow (c) and North Florida Strait, black arrow (d) during GOMECC3 cruise in Aug-Sep 2017.

5. Discussion

5.1 Currents and Eddy Kinetic Energy

Floats and moored current meters were deployed throughout the Gulf from July 2011 to June 2015 to better understand circulation in the Gulf and to calculate eddy kinetic energy (EKE) and mean kinetic energy (MKE) in the Gulf as shown in Figure 11 (after Perez-Brunius et al., 2018). The highest EKE was in the eastern Gulf area where the LC moves into the Gulf through the Yucatan Channel and out of the Gulf through the Straits of Florida. While this is an area with limited historical or recent deep PM data, it contains interesting features and conditions that relate to nepheloid layers. Strong currents, erosional furrows and high values in near bottom PM have been observed as discussed in the Background and Results sections.

The station at 25.5°N, 88° W in Figure 6h (also marked by black diamonds on Figures 12b and by black line in 12d) has elevated c_p values near the bottom in the area where surface EKE is high (Figure 11). At station 4-106 (Figure 9), which is located near the center of the high EKE region (rightmost white star in Figure 11), PM concentration reached ~550 µg l^{-1} near the seafloor.

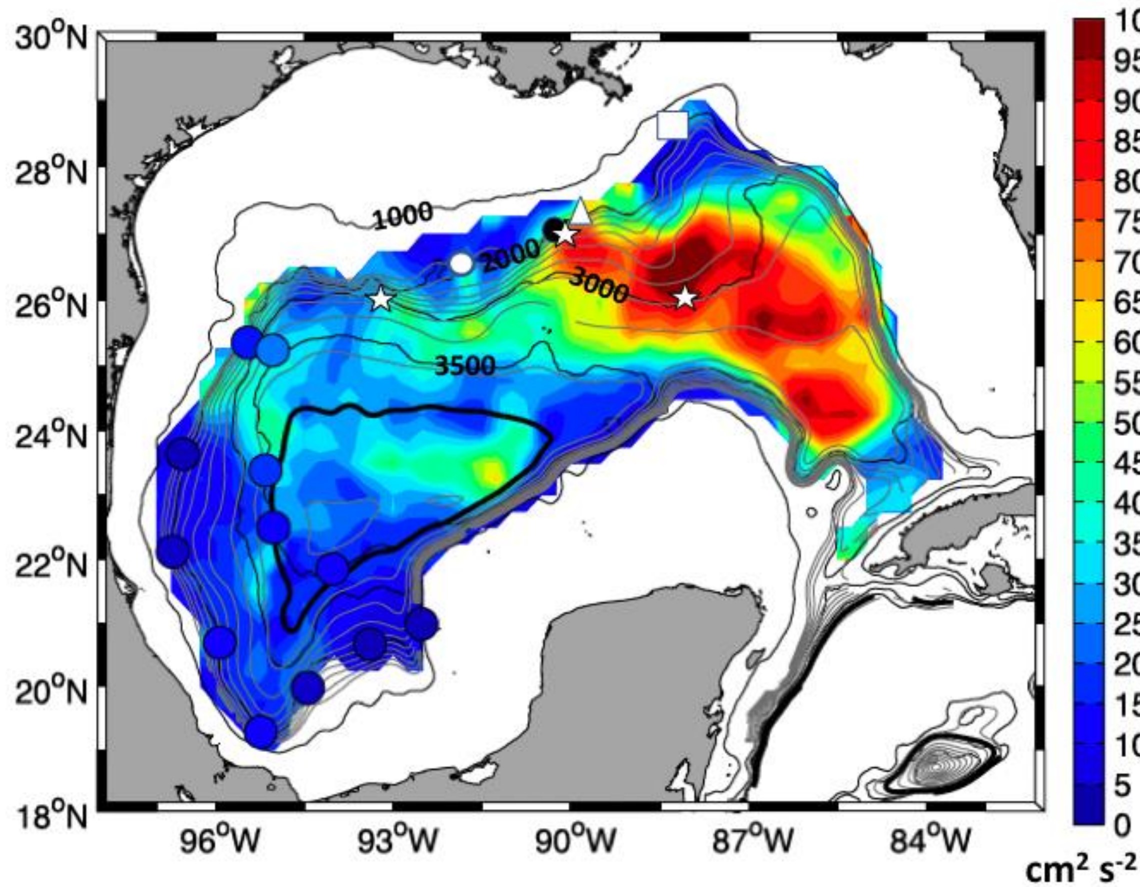

Figure 11. EKE (cm^2 s^{-2}) based on data from floats (color map) and moorings (large blue-colored dots) from 2011 to 2015. The white triangle is the location of Hamilton and Lugo-Fernandez (2001) current meter measurements (Figure 3). The black dot is the location of Green Knoll (Figure 4). The white circle is the location of Feely (1975) profiles in different years (Figure 13). Diercks et al., (2018) studied currents and nepheloid layers near the white square. The three white stars are locations of the three stations during 2021 (West to East: stations 4-73, 4-37 and 4-106 in Figure 9). Figure modified from Perez-Brunius et al., 2018, figure 5a.

Between August 2008 and August 2010, bottom current speed events of 10-40 cm s^{-1} were measured around the Gulf of Mexico in between anticyclonic-cyclonic pairs using point current meters at depths of 1000 m to 3500 m on seven moorings that also had a downward-looking Acoustic Doppler Current Profiler mounted at 20 mab (Kolodziejczyk et al., 2012). In the eastern Gulf of Mexico, the high-speed events occurred along the edge of the LC between its anticyclonic circulation and a nearby cyclonic eddy. Five years of current measurements throughout the water column in the western Gulf of Mexico indicated that the westward movement of detached LCE strongly modulate not only the upper-layer circulation but also impact the deep flow with currents up to 10-20 cm s^{-1} (Tenreiro et al., 2018). Based on Miller et al. (1977), these current speeds are sufficient to cause the weak (Figure 6i; 2017) to moderate (Figure 6h; 2016) to strong (Figure 6g; 2015) nepheloid layers found in the western Gulf.

5.1 Interannual variability of Gulf nepheloid layers

A comparison among the three years of XIXIMI data (green c_p profiles in Figure 12 c, d, g) clearly shows that deep nepheloid layers were much stronger in 2015 and 2016 than in 2017. A similar comparison between 2015 or 2016 with 2021 values of c_p in Figure 12 (c, d, h) shows that nepheloid layers were much stronger in central locations in 2021 than in 2017.

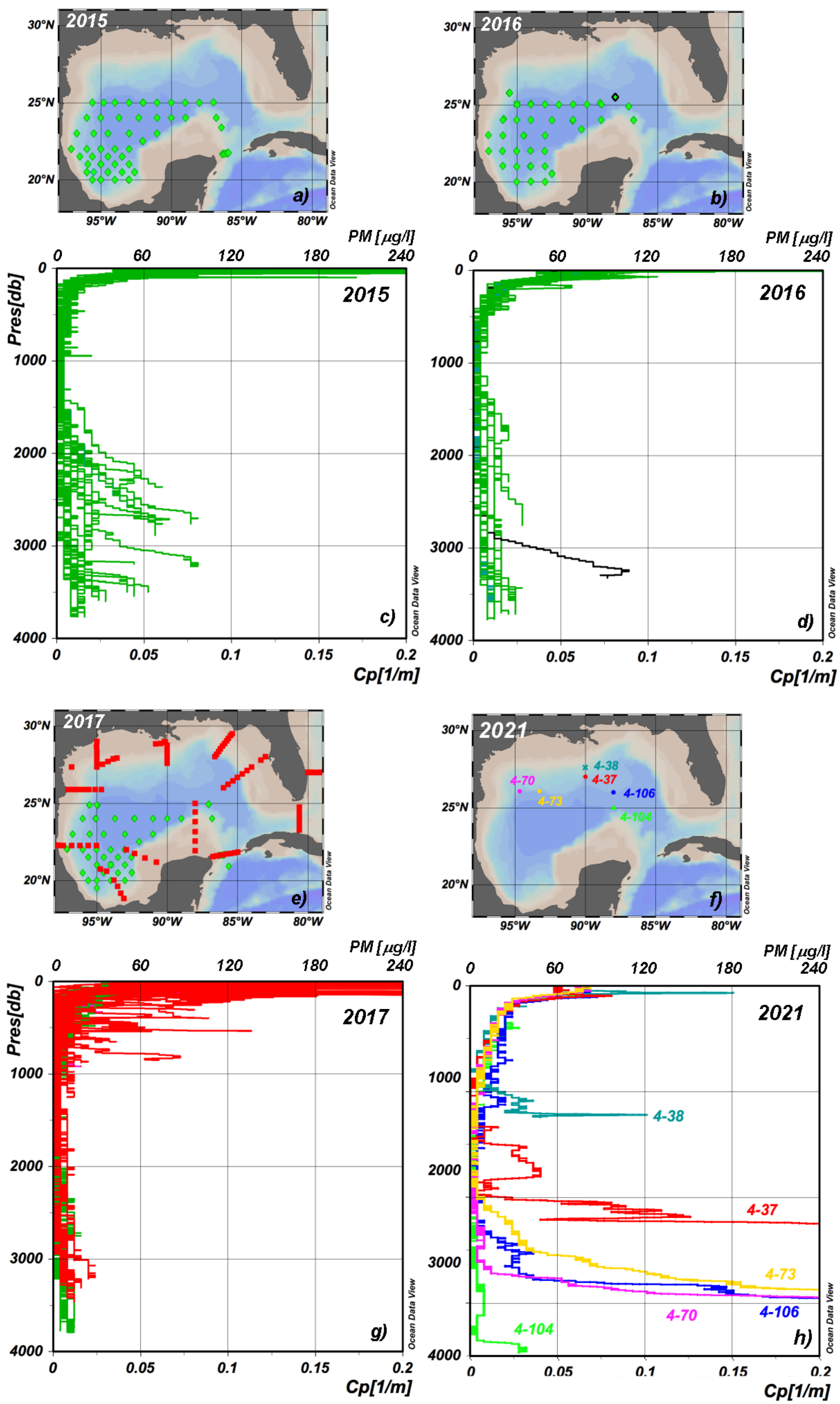

2015
30°N
25°N
20°N
95°W
90°W
85°W
80°W
a)
Ocean Data View
2016
b)
PM [µg/l]
0
60
120
180
240
Pres[db]
0
1000
2000
3000
4000
2015
c)
0
0.05
0.1
0.15
0.2
Cp[1/m]
2016
d)
2017
e)
2021
4-38
4-37
4-70
4-73
4-106
4-104
f)
2017
g)
2021
4-38
4-37
4-73
4-70
4-106
4-104
h)

Figure 12. Variability of the c_p/PM profiles during summer/fall seasons from 2015 to 2021 in the GOM a) and c) – XIXIMI4 cruise, 2015; b) and d) – XIXIMI5 cruise, 2016; e) and g) – XIXIMI6 and GOMECC3 cruises, 2017; f) and h) – 2021 expedition (colored symbols and profiles marked with station numbers). Green dots and profiles - XIXIMI data;.red dots and profiles - GOMECC3 data; black symbol and profile in b) and d) denote an anomalous station (see text for details). The 2021 profiles (panel h) are shown on full scale in Figure 9a.

With the exception of the 2021 data where PM concentrations exceeded 400 µg l^{-1} (Figure 9) the most intense benthic nepheloid layers in the deep Gulf appeared during 2016 on the central abyssal plain (Figure 6h; 88°W max c_p = 0.08 m^{-1} (PM~100 µg l^{-1})) and lower slopes in the western Gulf (Figure 6g; max c_p = 0.07 m^{-1} (PM~85 µg l^{-1})), but the c_p distribution in the three summer snapshots was highly variable, showing no consistent patterns (Figure 6g-i). This is in stark contrast to the consistency of c_p distribution in decadal repeat sections observed in Atlantic, Pacific, and Indian Oceans (Gardner et al., 2018a). Most of the area sampled during the three summers had bottom c_p of <0.03 m^{-1} (PM~36 µg l^{-1}). The sporadic appearance of nepheloid layers along 24°N in Figure 6 might result from the unpredictable intensification of bottom currents between cyclonic-anticyclonic eddy pairs moving westward as observed by Kolodziejczyk et al., 2011, 2012, and Tenreiro et al., 2018. We expect that the thick nepheloid layers (Figures 6 and 12) are not due to vertical mixing but rather are due to sediment resuspension further upslope with lateral advection and mixing (Armi, 1978; Gardner et al. 1985; McCave, 1986; Turnewitsch et al., 2013). Examples of vertical nepheloid layer concentration reversals that are interpreted as laterally advected detached mixed layers (intermediate nepheloid layers) are shown by McCave (1983).

EKE diminishes toward the western Gulf as the detached LCEs move westward and dissipate energy. There was no temporal overlap between published current measurements and c_p profiles during any of the cruises, but the four-year average of EKE data are useful for understanding mean long-term conditions on a broad geographic scale. We also examine where strong currents or strong nepheloid layers have been observed in previous studies to look for possible connections and causes of anomalous events. One must remember that single profiles represent just a short moment in time, and because of the dynamic nature of LCEs and their potential link with nepheloid layers, single profile measurements are not always likely to represent years-long EKE averages based on data from profiling floats and moored measurements shown in Figure 11. For example, compare the differences in PM concentrations in Figure 8a-c at stations 3-22 (max ~ 15 µg l^{-1}) versus 4-38 (~120 µg l^{-1}) and 3-54 (max ~25 µg l^{-1}) versus 4-70 (max ~440 µg l^{-1}); pairs taken in the same locations 4 years apart. Simultaneous long time-series measurements of both currents and c_p are needed to better connect the causes and effects of nepheloid layers (e.g. Gardner et al., 2017).

While PM data analyzed from five cruises lack temporal or spatial synchroneity with current measurements, they demonstrate that measured c_p values and PM concentrations are consistently high on the shelf (c_p >0.1 m^{-1}, 120 µg l^{-1}) and upper slope (c_p >0.07 m^{-1}, 85 µg l^{-1}) and generally low to very low (c_p <0.03 m^{-1}, 35 µg l^{-1}) in the deep basins. However, data from previous studies in other parts of the Gulf show exceptionally high and variable bottom PM concentrations and/or currents, providing evidence of sufficiently strong currents in some areas to cause active erosion of the seafloor (Feely et al. 1974; Feely, 1975; Hamilton and Lugo-Fernandez (2001); Diercks et al., 2018).

Southwest of the site where these strong oscillating currents in Figure 3 were measured (at white triangle in Figure 11), Feely et al., (1974) and Feely (1975) filtered water samples collected between depths of 1000 m to 2000 m (at white dot in Figure 11) that yielded particle concentrations up to 300 µg l^{-1} at 200 mab in 1971 (Figure 13). The fact that the PM maximum was at 200 mab indicates that the sediment was eroded at a shallower depth and was advected/transported to this location. How far away erosion occurred is not known. In 1973, the PM concentrations at the same location were only 10-25 µg l^{-1}. This order of magnitude difference is consistent with the large southwest-northeast velocity variations measured by Hamilton & Lugo-Fernandez (2001) (Figure 3). It is also consistent with the statement by Tenreiro et al., (2018) that the detached anticyclonic LCEs strongly impact both the upper-layer circulation and the deep flow along the slope as they move westward. Long time-series synchronous measurements of current speeds and PM concentrations in multiple locations near the furrows and the Sigsbee Escarpment could help to better understand the driving forces of this system and the relationship among detached LCEs, eddy-topography interactions, topographic Rossby waves and sediment resuspension and transport.

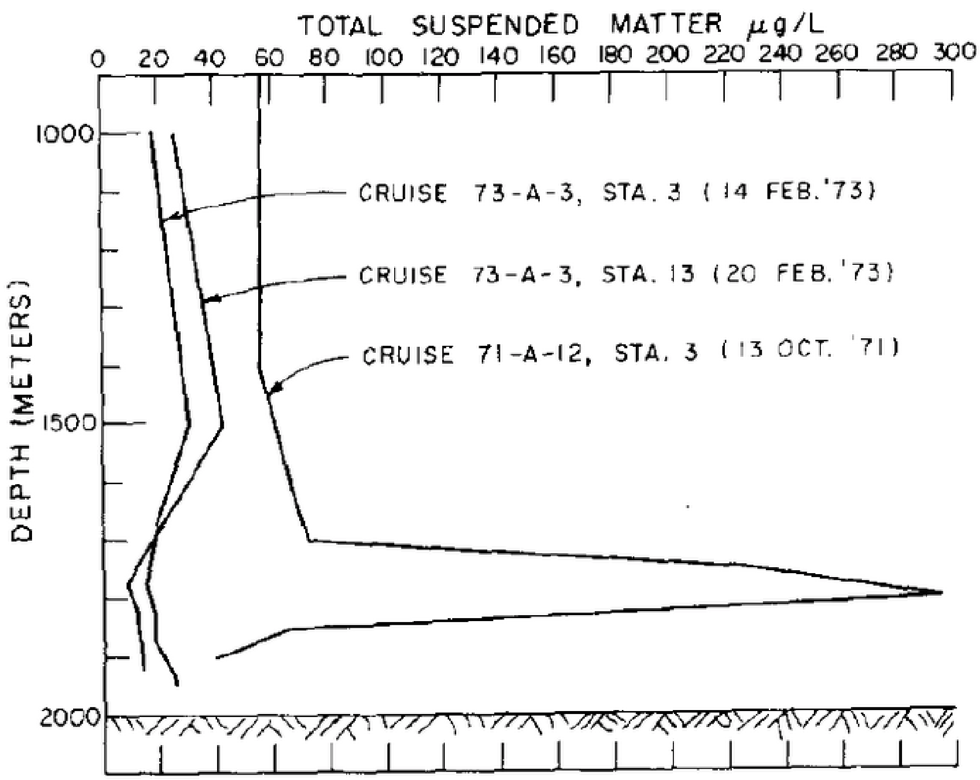

Figure 13. Profiles of PM filtered from water samples collected at the location marked by white circle in Figure 11 (Feely et al., 1974; Feely, 1975).

5.3 Nepheloid layers in the incoming (Yucatan Channel) and outgoing channels (Straits of Florida) of the Gulf of Mexico.

Sections of c_p across the Yucatan Channel and South/North Straits of Florida showed minimal nepheloid layers in the deepest parts of the channels (Figure 10). Transport through the Yucatan Channel varies seasonally with the highest values in the summer when transport is 20-40% higher than the mean transport (Athie et al., 2020). Summer was the season when the c_p data were collected, so the high-transport summertime is when sediment resuspension would be most likely. However, Athie et al. (2020) did not provide data on near-bottom current velocity, which is the driving force for creating nepheloid layers. Sediment in these passages has a higher percentage of carbonate material and lower percentage of fine-grained terrigenous sediment (Davis, 2017, figures 3.16 and 3.17). Much of the fine terrigenous sediment has been winnowed away over time, and the larger carbonate particles and substrate are more difficult to erode and resuspend to create and sustain nepheloid layers.

Bottom currents beneath the Gulf Stream east of Florida sometimes flow south for periods of 4-6 days on the western side of the Strait (Düing and Johnson, 1972; Düing, 1975). Southerly currents measured from a submarine near the seafloor sometimes exceeded 50 cm s^{-1} (Gardner et al., 1989) and reached 87 cm s^{-1}, as recorded by moored current meters (Düing, 1975). Wimbush and Lescht (1979) measured currents at 3 mab and filmed sediment transport in the Florida Straits. They reported irregular sediment ripple transport when currents reached 22-24 cm s^{-1}.

Near-bottom currents measured in the Yucatan Channel yielded a mean flow of about 2 cm s^{-1} (Sheinbaum et al., 2002), although the flow in their year-long measurements showed some reversals in its direction between the Caribbean basin and the Gulf. Unfortunately, time series of current speeds were not provided.

6. Conclusions.

While it is well known that nepheloid layers are often strong on the shelf and upper slope in the Gulf of Mexico, especially near river outflows around the Gulf, new data presented here reveal weak to strong nepheloid layers (15 – 120 µg l^{-1}) deeper than 2500 m in the southwestern area of the Gulf in summers of 2015-2017. The data collected in 2021 demonstrate that there are locations/times such as near furrows and in areas of high EKE where nepheloid layer PM concentrations can reach extremely high values: 500 - 1400 µg l^{-1}.

Studies in major oceans have found that areas of high surface EKE are often related to areas of strong nepheloid layers. Although there were no simultaneous measurements of currents or eddy kinetic energy (EKE) and c_p (a proxy for PM) during our Gulf studies, our observations show that moderate (10's – 100 µg l^{-1}) nepheloid layers were observed in varying locations at depths over 1200 m each summer. The shifting nepheloid layers are possibly associated with intensified deep currents created by detached Loop Current anticyclonic eddies or between cyclonic and anticyclonic eddies moving west in the Gulf. The irregular western drift of these eddies may explain the observed lack of interannual consistency of where elevated currents and nepheloid layers occur.

Near-bottom PM concentrations were barely elevated in the Yucatan Channel or Florida Straits, suggesting minimal transport of fine sediment through the channels at that time (summer 2017).

The presence of very strong currents and a strong nepheloid layer near large furrows in the northern Gulf slope indicate conditions of active sediment erosion, resuspension, and transport. More long-term, simultaneous measurements of currents and near-bottom PM concentrations in strategic locations in the Gulf of Mexico would aid in understanding the dynamics of currents and large furrows and the relationship between nepheloid layers and EKE in the Gulf of Mexico.

Data availability: Finalized transmissometer data are freely and openly available in c_p units (m^{-1}) through Ocean Data View Repository (https://odv.awi.de/en/data/ocean/global-transmissometer-database/). Availability of the finalized GOMECC3 is at https://cchdo.ucsd.edu/cruise/33RO20170718.

Acknowledgements:

We thank the captains and crews of Mexico's B/O Justo Sierra and the NOAA ship R/V Ron Brown, and the scientists aboard those vessels for collecting data during the XIXIMI4, 5, 6 and GOMECC cruises. We thank Reiner Schlitzer for continuous development of Ocean Data View software that we use for data analyses and figure compilations. Reviewers are thanked for their questions and suggestions that have helped us more clearly present the data.

Funding: The research on Mexico's research vessel was conducted with funding from the Mexican National Council for Science and Technology—Mexican Ministry of Energy—Hydrocarbon Fund (project 201441). This is a contribution of the Gulf of Mexico Research Consortium (CIGoM) who acknowledge PEMEX's specific request to the Hydrocarbon Fund to address the environmental effects of oil spills in the Gulf of Mexico. Funding for the GOMECC cruises came from the NOAA Ocean Acidification Program (OAP) and we thank Drs. Leticia Barbero and Molly Baringer for the CTD data. Analysis and synthesis of these data have been supported by: US National Science Foundation (contract OCE-1536565 to Gardner and Richardson), NOAA (grant NA19NES4320002 to Mishonov at Cooperative Institute for Satellite Earth System Studies - CISESS) at the University of Maryland/ESSIC and NCEI/NOAA (both US), and support from the TAMU Earl F. Cook Professorship (Gardner).

References cited

Armi, L. (1978). Mixing in the deep ocean - the importance of boundaries. *Oceanus* 21, 14–19.

Athie, G., Sheinbaum, J., Candela, J., Ochoa, J., & Perez-Brunius, P. (2020). Seasonal variability of the transport through the Yucatan Channel from observations. *American Meteorological Society*, DOI: 10.1175/JPO-D-18-0269.1.

Baker, E. T., & Lavelle, J. W. (1984). The effect of particle size on the light attenuation coefficient of natural suspensions. *Journal of Geophysical Research 89*, 8197-8203.

Barbero, L., Pierrot, D., Wanninkhof, R., Baringer, M., Hooper, J., Zhang, J.Z., Smith, R., Byrne, R., Langdon, C., Hernández-Ayón, M., Schnetzer, A., Stauffer, B., Herzka, S., Compaire, J.C., Hernández, F., Pech, D., Hu, C., English, D., Ondrusek, M., Olascoaga, J., & Derr, G. (2019). Third Gulf of Mexico Ecosystems and Carbon Cycle (GOMECC-3) Cruise. Corporate Authors: Atlantic Oceanographic and Meteorological Laboratory, NOAA. DOI: https://doi.org/10.25923/y6m9-fy08.

Bean, D. A. (2005). Past and present deepwater contour-current bedforms at the base of the Sigsbee Escarpment, Northern Gulf of Mexico, 163 pp, PhD Dissertation, Texas A&M University, College Station, Texas.

Bernal, C. E. (2001). Spatial and temporal distributions of particulate matter and particulate organic carbon, northeast Gulf of Mexico, MS Thesis, 108 pp, Texas A&M University, College Station, Texas.

Bracco, A., Choi, J., Joshi, K., Luo, H., & McWilliams, J. C., (2016). Submesoscale currents in the Northern Gulf of Mexico: Deep phenomena and dispersion over the continental slope. *Ocean Modell*., 101, 43–58, https://doi.org/10.1016/j.ocemod.2016.03.002.

Brewer, P.G., Spencer, D.W., Biscaye, P.E., Hanley, A., Sachs, P.S., Smith, C.L., Kadar, S., & Fredericks, J. (1976). The distribution of particulate matter in the Atlantic Ocean. *Earth and Planetary Science Letters, 32,* 393–402.

Bryant, W., Bean, D. A. Slowey, N. C., Dellapenna, T. M., & Scott, E. (2001). Deepwater currents form mega-furrows near US Gulf's Sigsbee Escarpment, *Offshore Magazine* (Conroe, Texas).

Cochran, E. M. (2013). The role of particulate matter in the development of hypoxia on the Texas-Louisiana shelf, MS Thesis, 106 pp, Texas A&M University, College Station, Texas.

Coleman, J. M. (1988). Dynamic changes and processes in the Mississippi River delta. *Geological Society of America Bulletin, 100*, 999–1015.

Davis, R. A. (2017). Sediments of the Gulf of Mexico, in *Habitats and Biota of the Gulf of Mexico: Before the Deepwater Horizon Oil Spill: Volume 1: Water Quality, Sediments, Sediment Contaminants, Oil and Gas Seeps, Coastal Habitats, Offshore Plankton and Benthos, and Shellfish*, edited by C. H. Ward, pp. 165-215, Springer New York, New York, NY, doi:10.1007/978-1-4939-3447-8_3.

Diercks, A.R., Dike, C., Asper, V.L., DiMarco, S.F., Chanton, J. P., & Passow, U. (2018). Scales of seafloor sediment resuspension in the northern Gulf of Mexico. *Elementa Science of the Anthropocene*, 6: 32. DOI: https://doi.org/10.1525/elementa.285.

DiMarco, S. F., Reid, R. O., & Nowlin, Jr. W. D., (2005). A Statistical Description of the Near-surface Velocity Field from Drifters in the Gulf of Mexico. Geophysical Monograph Series, Volume 161, Circulation of the Gulf of Mexico: Observations and Models. Eds. W. Sturges and A. Lugo-Fernandez. American Geophysical Union, pp. 101 - 110.

Dixon, K.W., Delworth, T.L., Rosati, A.J., Anderson, W., Adcroft, A., Balaji, V., Benson, R., Griffies, S.M., Lee, H-C., Pacanowski, R.C., Vecchi, G.A., Wittenberg, A.T., Zeng, F., Zhang, R. (2011). Ocean circulation features of the GFDL CM2.6 & CM2.5 high-resolution global coupled climate models. In: WCRP Open Science Conference. Denver, Colorado.

Düing, W.O. (1975). Synoptic studies of transients in the Florida current. *Journal of Marine Research*, 33: 53-73.

Düing, W.O. & Johnson, D.R. (1972). High resolution current profiling in the Straits of Florida. *Deep-Sea Research*, 19: 259-274.

Feely, R. A. (1975). Major-element composition of the particulate matter in the near-bottom nepheloid layer of the Gulf of Mexico. *Marine Chemistry*, 3, 121-156.

Feely, R. A., Sullivan, L., & Sackett, W. M. (1974). Light scattering measurements and chemical analysis of suspended matter in the near bottom nepheloid layer of the Gulf of Mexico, 281-293 pp., Plenum Press, New York.

Gardner, W. D., Biscaye, P. E., Zaneveld, J. R. V. & Richardson, M. J. (1985). Calibration and comparison of the LDGO nephelometer and the OSU transmissometer on the Nova Scotian Rise. *Marine Geology*, 66:323-344.

Gardner, W.D., Blakey, J.C., Walsh, I.D., Richardson, M.J., Pegau, S., Zaneveld, J.R.V., Roesler, C., Gregg, M.C., MacKinnon, J. A., Sosik, H.M., & Williams, III, A.J. (2001). Optics, particles, stratification and storms on the New England continental shelf. *Journal of Geophysical Research*, 106: 9473-9497.

Gardner, W.D., Tucholke, B.E., Richardson, M.J., & Biscaye, P.E. (2017). Benthic storms, nepheloid layers, and linkage with upper ocean dynamics in the Western North Atlantic. *Marine Geology*, *385*, 304-327. http://dx.doi.org/10.1016/j.margeo.2016.12.012.

Gardner, W.D., Mishonov, A.V., & Richardson, M.J., 2018a. Decadal Comparisons of Particulate Matter in Repeat Transects in the Atlantic, Pacific, and Indian Ocean Basins, Geophysical Research Letters 45 (1), 277-286. https://doi.org/10.1002/2017GL076571

Gardner, W.D., Richardson, M.J., & Mishonov, A.V. (2018b). Global assessment of benthic nepheloid layers and linkage with upper ocean dynamics. *Earth and Planetary Science Letters, 482*, 126–134, https://doi.org/10.1016/j.epsl.2017.11.008.

Gardner, W. D., Richardson, M. J. & Cacchione, D. A. (1989). Sedimentological effects of strong southward flow in the Straits of Florida. *Marine Geology,* 86:155-180.

Gray, R. M. (2016). Influences on the temporal and spatial variability of particulate matter in the northern Gulf of Mexico, MS Thesis, 104 pp, Texas A&M University, College Station, Texas.

Hamilton, P. (2007). Deep-current variability near the Sigsbee Escarpment in the Gulf of Mexico. *Journal of Physical Oceanography* 37, 708-726.

Hamilton, P., 2009. Topographic Rossby waves in the Gulf of Mexico. *Progress in Oceanography*, 82, 1–31, https://doi.org/10.1016/j.pocean.2009.04.019.

Hamilton, P., Donohue, K., Hall, C., Leben, R. R., Quian, H., Sheinbaum, J., & Watts, D. R. (2014). Observations and Dynamics of the Loop Current. U.S. Department of the Interior, Bureau of Ocean Energy Management, Gulf of Mexico OCS Region, New Orleans, LA, OCS Study BOEM 2015-006: 417 pp.

Hamilton, P., & Lugo-Fernandez, A. (2001). Observations of high speed deep currents in the northern Gulf of Mexico. *Geophysical Research Letters*, 28, 2867–2870. https://doi.org/10.1029/2001GL013039.

Kolodziejczyk, N., Ochoa, J., Candela, J., & Sheinbaum, J. (2011). Deep Currents in the Bay of Campeche, *Journal of Physical Oceanography*, 41: 1902-1920. DOI: 10.1175/2011JPO4526.1.

Kolodziejczyk, N., Ochoa, J., Candela, J., & Sheinbaum, J. (2012). Observations of intermittent deep currents and eddies in the Gulf of Mexico. *Journal of Geophysical Research*, 117, C09014, doi:10.1029/2012JC007890.

Leben, R. R. (2005). Altimeter-derived Loop Current metrics. Circulation in the Gulf of Mexico, *Geophysical Monograph*, Vol. 161, *American Geophysical Union*, 181–201, https://doi.org/10.1029/161GM15.

Lee, H.-C. (2003). Numerical simulation of the Gulf Stream System: The Loop Current and the deep circulation. *Journal of Geophysical Research,* 108, 3043, https://doi.org/10.1029/2001JC001074.

Linacre, L., Durazo, R., Camacho-Ibar, V. F., Selph, K. E., Lara-Lara, J. R., & Mirabal-Gómez, U. (2019). Picoplankton carbon biomass assessments and distribution of Prochlorococcus ecotypes linked to loop eddies during summer in the Southern Gulf of Mexico. *Journal of Geophysical Research: Oceans,* 124, 8342-8359, https://doi.org/10.1029/2019JC015103.

Maslo, A., Correia, J. M. A., & Pardo, J. S., (2020). Energetics of the Deep Gulf of Mexico, *Journal of Physical Oceanography*, 50; 1655–1675. https://doi.org/10.1175/JPO-D-19-0308.1.

McCave, I. N. (1983). Particulate size spectra, behaviour and origin of nepheloid layers over the Nova Scotian Continental Rise. *Journal of Geophysical Research*, 124: 7647-7666.

McCave, I. N. (1986). Local and global aspects of the bottom nepheloid layers in the world ocean. *Netherlands Journal of Sea Research,* 20, 167–181.

Miller, M. C., McCave, I. N., & Komar, P.D. (1977). Threshold of sediment motion under unidirectional currents. *Sedimentology,* 24, 507–527.

National Academies of Sciences, Engineering, and Medicine (2012). Approaches for Ecosystem Services Valuation for the Gulf of Mexico After the Deepwater Horizon Oil Spill: Interim Report. Washington, DC: The National Academies Press. https://doi.org/10.17226/13141.

National Academies of Sciences, Engineering, and Medicine (2018). Understanding and Predicting the Gulf of Mexico Loop Current: Critical Gaps and Recommendations. Washington, DC: *The National Academies Press*. https://doi.org/10.17226/24823.

Oey, L.-Y., Ezer, T. & Lee, H.-C. (2005). Loop Current, rings and related circulation in the Gulf of Mexico: A review of numerical models and future challenges. In *Circulation in the Gulf of Mexico: Observations and Models*. Edited by Sturges W. & Lugo Fernández, A. Washington, D.C. *Geophysical Monograph,* Vol. 161, American Geophysical Union, 31–56, https://doi.org/10.1029/161GM04.

Oey, L.-Y., & Lee, H.-C. (2002). Deep eddy energy and topographic Rossby waves in the Gulf of Mexico. *Journal of Physical Oceanography*, 32, 3499–3527, https://doi.org/10.1175/1520-0485(2002)032,3499:DEEATR.2.0.CO;2.

Pérez-Brunius, P., Furey, H., Bower, A., Hamilton, P., Candela, J., Garcia-Carrillo, P. & Leben, R. (2018). Dominant Circulation Patterns of the Deep Gulf of Mexico. *Journal of Physical Oceanography*. 48, 511-529. DOI: 10.1175/JPO-D-17-0140.1.

Schlitzer, R. (2021). Ocean Data View, https://odv.awi.de.

Sheinbaum, J., Candela, J., Badan, A., & Ochoa, J. (2002). "Flow structure and transport in the Yucatan Channel." Geophysical Research Letters 29, no. 3:10-1–10-4.

Shideler, G. L. (1981). Development of the benthic nepheloid layer on the south Texas Continental Shelf, western Gulf of Mexico, *Marine Geology*, 41, 37-61.

Southard, J. & Cacchione, D. (1972). Experiments on bottom sediment movement by breaking internal waves: in Swift, D., D. Duane & O. Pilkey: Shelf Sediment Transport-Process and Pattern, Dowden, Hutchinson and Ross, Inc. Stroudsburg, PA, p. 83—97.

Tenreiro, M., Candela, J., Pallàs Sanz, E., Sheinbaum, J., & Ochoa, J. (2018). Near-Surface and Deep Circulation Coupling in the Western Gulf of Mexico. *Journal of Physical Oceanography*, 48, 145-161. DOI: 10.1175/JPO-D-17-0018.1.

Turnewitsch, R., Falahat, S., Nycander, J., Dale, A., Scott, R. B., Furnival, D. (2013). Deep-sea fluid and sediment dynamics—influence of hill- to seamount-scale seafloor topography. *Earth Science Reviews*, 127, 203–241.

Wimbush, M., & Lescht, B. (1979). Current-induced sediment movement in the deep Florida Straits: critical parameters. *Journal of Geophysical Research,* 84, 2495-2502.

Wunsch, C. (2015). Modern Observational Physical Oceanography, Understanding the Global Ocean. Princeton University Press, ISBN. 9780691158822. 512 pp.

Zhang, Y. (1997). Sedimentation and resuspension across the central Louisiana inner shelf. 205 pp. Texas A&M University, College Station, Texas.

Zuck, N. A. (2014). The relationships of particulate matter and particulate organic carbon with hypoxic conditions along the Texas-Louisiana shelf. 96 pp, Texas A&M University, College Station, Texas.